

Portable Laser Guided Robotic Metrology System

Peter A. Slater, James M. Downey, Marie T. Piasecki, Bryan L. Schoenholz
NASA Glenn Research Center
Cleveland, Ohio, United States of America
peter.slater@nasa.gov

Abstract—This paper introduces the new Portable Laser Guided Robotic Metrology (PLGRM) system at the National Aeronautics and Space Administration’s (NASA) Glenn Research Center. Previous work used industrial robots in fixed facilities to characterize antennas and required fixtures that do not lend themselves to portable applications. NASA’s PLGRM system is designed for in-situ antenna measurements at a remote site. The system consists of a collaborative robot arm mounted on a vertical lift and a laser tracker, each on a mobile base. Together, they enable scanning a surface larger than the robot’s reach. To accomplish this, the robot first collects all points within its reach, then the system is moved and the laser tracker is used to relocate the robot before additional points are captured. The PLGRM implementation will be discussed including how safety and planning are combined to effectively characterize antennas. Software defined triggering is a feature, for flexible integration of vector network analyzers and antenna controllers. Lastly, data will be shown to demonstrate system functionality and accuracy.

I. INTRODUCTION

The National Aeronautics and Space Administration’s (NASA) Glenn Research Center is investigating alternatives to antenna ranges for in-situ measurements of phased array antennas embedded on an aircraft. Moving the aircraft and antenna under test (AUT) to existing chambers is challenging, due to the costs and the limited availability of sites. A portable system may be able to address these concerns. This paper discusses the development of a Portable Laser Guided Robotic Metrology (PLGRM, pronounced pil-grim) system for Ku-band near-field (NF) and far-field (FF) antenna measurements.

A portable NF system exists [1] but is heavy and dependent on a crane being provided and modified. This was not possible for our application, as we were required to be more portable. First, components had to be easily shipped and assembled by two people. Second, the PLGRM cannot impose any requirements or modifications of the host facility. Therefore, the system cannot be anchored to the floor and must run off of commonly available 110 VAC wall power with unknown quality. Finally, as the system is unconstrained, it should sense collisions and minimize the risk of damaging the AUT or aircraft.

Multiple groups have demonstrated the flexibility of industrial robots to perform both NF and FF measurements [2]–[6]. However, these systems are not portable. The National Institute of Standards and Technology (NIST) has summarized the key issues that were identified in the designs of their robotic antenna ranges [7].

The first is that industrial robots are repeatable, not accurate and require correction to enable measurements at higher frequencies. There are two methods of correction: calibration and closed loop control, and achieving the best accuracy requires both [8]. The feedback for both these methods is commonly provided by photogrammetry [4] or a laser tracker [9]. Our work is to adapt the measurement flexibility of robotics to also be portable.

Our paper is outlined as follows. Section II goes over the component choices and how the portability requirement was met. Implementation is discussed in III and preliminary measurements are reviewed in IV.

II. COMPONENTS

The first two portability requirements were met by selecting a light weight, collaborative robot. Limitations of the robot size were overcome by integration with a vertical lift and a mobile base to extend the reach. The radio frequency (RF) measurement components were specifically affected by the third requirement on power. Figure 1 provides an overview of the components used, note that any mentions of products is not an endorsement and is done to clarify what was done in this work.

A. UR10 Collaborative Robot

Collaborative robots or “cobots” are industrial robots combined with safety systems that are certified to operate in close proximity with humans. This is important given the unconstrained movement of a robotic arm, not for human safety, but for protection of the AUT and aircraft.

A Universal Robots UR10 robotic arm was used because it met the size, power, and safety requirements; albeit with a limited reach of 1.3 meters [10]. The UR10 end-effector can carry a payload mass of 10 kilograms, which is sufficient for the light weight pyramidal horns and open ended waveguide probe antennas used at Ku frequencies. Our current payload mass is 4 kilograms, leaving plenty of room for heavier probes.

B. LIFTKIT and Mobile Base

The UR10’s 1.3 meter reach was an issue as the AUT-size required a far-field radius of about 1.7 meters [11]. The solution was to use a mobile base and a SKF Motion Technologies LIFTKIT with a 900 millimeter stroke. Together they extend the UR10’s reach from zero to three meters vertically, and with a method described in III-B, an arbitrary reach in other directions. Although now external feedback is required to maintain accuracy.

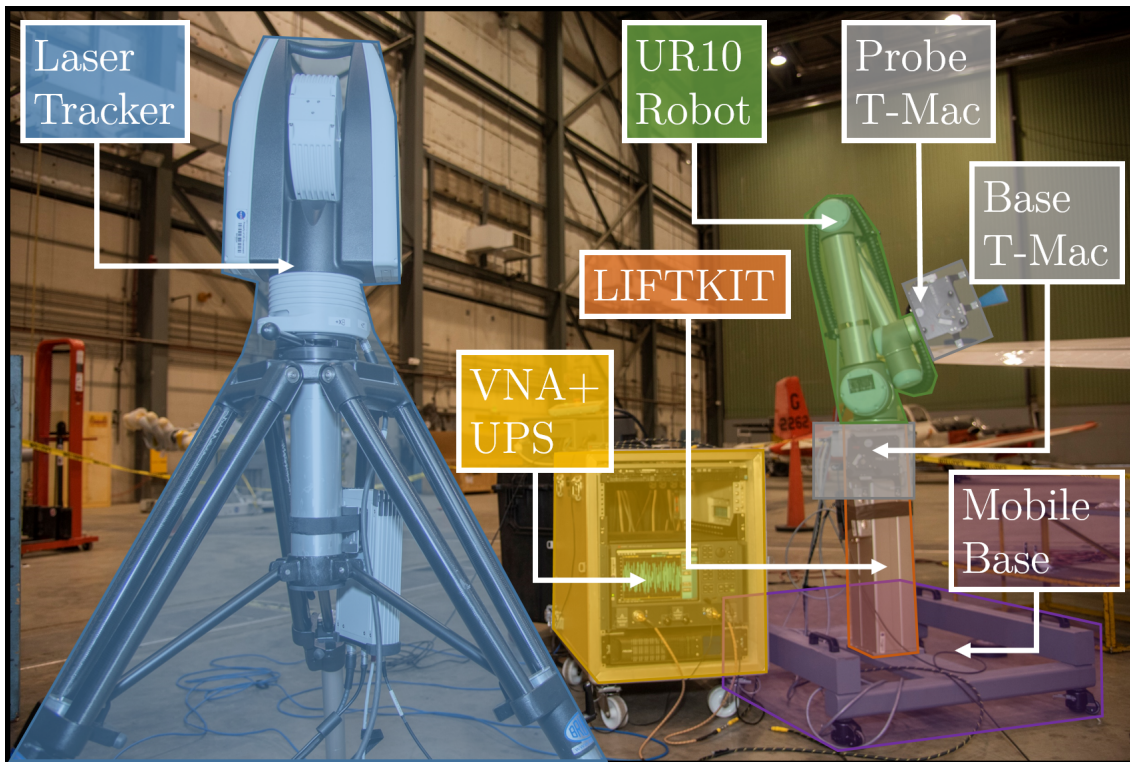


Fig. 1: The PLGRM system configured for antenna measurements. The UR10 robotic arm is mounted on a vertical LIFTKIT and a mobile base to extend the robot’s reach. The laser tracker and Base/Probe T-Macs were used to maintain accuracy. The vector network analyzer (VNA) was integrated with an uninterruptible power supply (UPS) to be robust to low quality power.

C. Laser Tracker

Both laser trackers and photogrammetry can be used to provide accurate position feedback. The big difference is performance, a laser tracker [12] can provide measurements faster and with lower latency than photogrammetry [13]. This performance is needed for online control of a robotic arm.

A Leica AT960 laser tracker was used with six degree of freedom (6DOF) T-Mac targets. In a 6DOF measurement, both the T-Mac position and orientation is captured simultaneously. Another target type, called spherically mounted retroreflectors (SMR), only captures the position.

The final target is the handheld 6DOF T-Probe, not to be confused with the probe antenna or the Probe T-Mac. It is used for measuring points at the end of a stylus, which are often not visible to the laser tracker. Three offsets are measured with the T-Probe: the Base T-Mac to the robot base, the Probe T-Mac to robot end-effector, and the Probe T-Mac to probe antenna. Offsets are used to convert corresponding T-Mac measurements into the point of interest (i.e. the robot base and the probe antenna aperture).

During setup, the laser tracker measures a constellation of stable SMRs to define an inertial coordinate system (ICS). The AUT is brought into the ICS by T-Probing its features and relating them to a separate constellation of SMRs on the aircraft. After moving the laser tracker or aircraft, their constellations can be measured to relocate them in the ICS.

NIST’S CROMMA antenna range demonstrated the use of two Probe T-Macs for robot guidance [2]. The PLGRM also uses two, but only one is on the payload for robot guidance, the other is on the base. UR10 movements are commanded relative to its base, which is located in the ICS by measuring the Base T-Mac and applying the offset. The benefit of having the Base T-Mac is for quickly relocating the robot in the ICS after repositioning with the mobile base or LIFTKIT. Overall, the laser tracker provides fast and accurate AUT alignment; the AUT can be placed and moved as needed and the measurement system brought to it.

D. Vector Network Analyzer

Part of portability is dealing with the possibility of dirty, industrial power at the host facility. An uninterruptible power supply (UPS) was integrated with a Keysight PNA-X vector network analyzer (VNA) to provide stable power. The UPS provides clean power and allows for the VNA to be moved alongside the robot without shutting down, but with a significant increase in weight. Sometimes, to reduce weight, the PNA-X and UPS is substituted for a more portable Keysight FieldFox VNA with a built in battery. This substitution and much more is the product of a flexible Software Defined Triggering (SDT) system described in III-F.

III. IMPLEMENTATION

Measurements are started by providing an arbitrary set of points, either directly or sampled from a surface in Figure 2. It should be noted that a “point” implies both position and orientation in this paper. Points are then filtered to select those that are unmeasured, reachable, and visible. When points are not visible, a Virtual Point Method (VPM) is attempted to make the them visible (see III-C).

A simple path is then constructed through the remaining points before being passed to the controller to servo the robot to each point and stop. Once stopped, the Software Defined Triggering (SDT) specifies what actions occur. Benefits of this implementation are the extendability of SDT and the ability to restart failed or incomplete measurements.

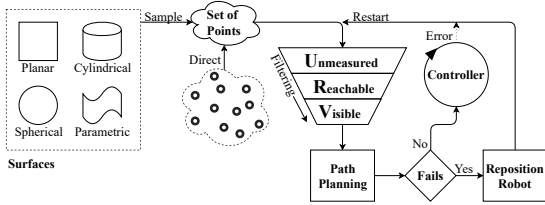


Fig. 2: Overview of the software implementation.

A. Collision Detection

Section II-A discussed the safety benefits of cobots. While it is important that the system stops after a collision, it is desired that it never collides in the first place. This requires both modeling the environment and simulating movements before sending them to the robot, together known as collision detection (CD). CD was implemented using oriented bounding boxes (OBB). Non-box shapes are wrapped with multiple boxes to provide a tight, but oversized model of OBB’s, as in Figure 3. The collision between collections of OBB’s can be computed efficiently [14]. Efficiency is important for both uses of CD: point filtering prior to a scan, due to the possibly large number of points, and for validating controller corrections before execution.

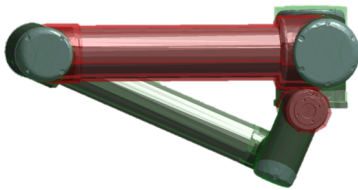


Fig. 3: Robot wrapped with OBB collision model. The color red indicates that the wrist and bicep are colliding.

B. Point Filtering

Repositioning requires the ability to filter which points to measure at a position and then be able to restart the measurement at the next position. The first step of filtering is to select the unmeasured points and the second step is to select the reachable points. The conversion from a desired point to joint angles is known as an inverse kinematics (IK) problem, for which the UR10 has an analytical solution [15]. The angles and current robot position are then used to update the collision model. A point is reachable if robot joint angles exist that gets the probe antenna to the point without collision. Unreachable points are eventually reached by using the mobile base and LIFTKIT to reposition the robot. With measurement restarting, this effectively gives the robot an arbitrarily large reach.

C. Virtual Point Method

The final step of filtering is to select points that are visible from the laser tracker. The Probe T-Mac has a 90 degree cone of visibility [12] and is visible when the origin of the laser tracker is within its cone. Some not visible points can be made visible with the Virtual Point Method (VPM); for example, the second, orthogonal polarization at a point.

The steps of the VPM are illustrated in Figure 4 but put simply, the point is virtualized by rotating an arbitrary amount about the robot’s 6th-axis such that virtual point is visible. Then the original point is reached by servoing to the virtual point, followed by a counteracting 6th-axis rotation. VPM accuracy is better than a blind move as it is corrected by the laser tracker, but worse than a truly visible point as there is uncertainty in both locating the 6th-axis center and the counteracting rotation. The degradation still remains to be quantified and it should be noted that the process of losing the T-Mac and reconnecting adds an additional three seconds per point.

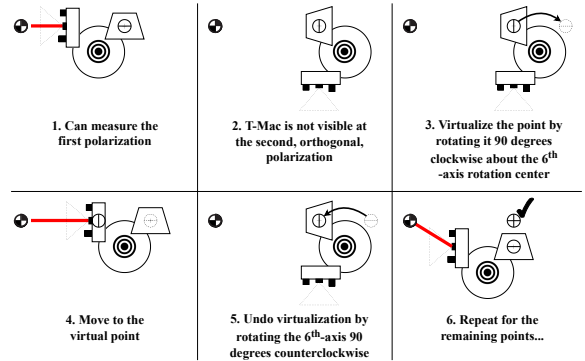


Fig. 4: Steps of the Virtual Point Method. The solid circle is the original point, where polarization is indicated by a dividing line. Similarly, the virtual point is a dashed circle. The centroid is the laser tracker origin, emitting a red laser beam if the target is visible. The spiky-rectangle is the Probe T-Mac with a dashed 90 degree visibility cone and the bullseye is the robot’s sixth axis rotation center. The trapezoid is the probe antenna, to be aligned with the point at both polarizations.

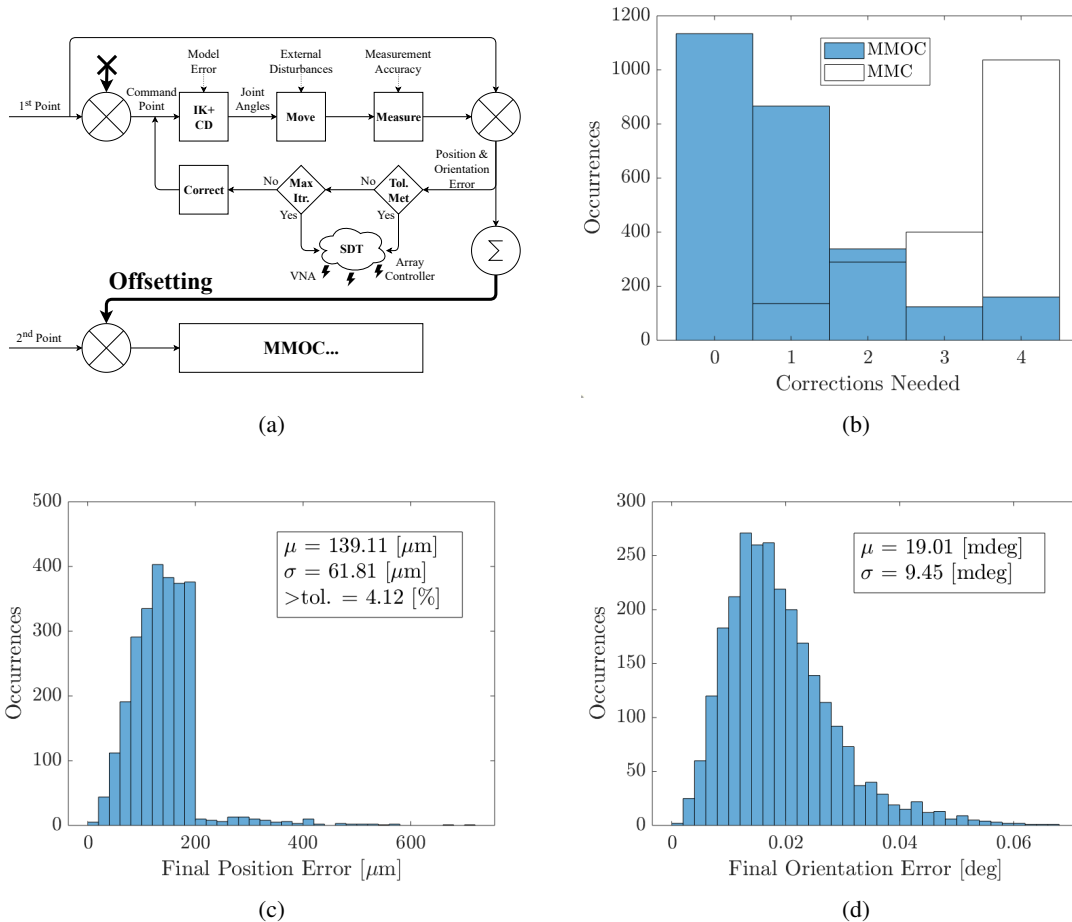


Fig. 5: MMOC controller overview. Controller performance was captured during a 5244 point planar near-field scan, plotted in Figure 7b. The controller was run with a maximum of five iterations (four corrections) and a position tolerance of 200 microns. Figure 5b is a histogram of the number of controller corrections needed to meet tolerances. Figures 5c and 5d are histograms of the final probe antenna position and orientation error, respectively.

D. Path Planning

A simple path is formed by visiting the unmeasured, reachable, visible (URV) points in the order given, often a zig-zag pattern. Then collision detection is performed at multiple steps between each point, where the step spacing is small enough to assume that there are no collisions between steps. If a collision is found going to a point, it is removed and the path moves onto the next point. Path planning fails if there are no URV points remaining, this is fixed by repositioning the robot and restarting the measurement. Once the path is formed, it is animated to provide the user a veto before it is sent to the controller.

E. Controller

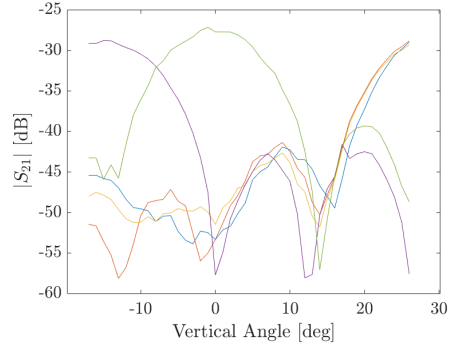
NIST introduced the move measure correct (MMC) algorithm [16]. For each iteration, the robot is moved to the desired point, the T-Mac measured, and then the joints corrected. Corrections are provided by the IK and verified by CD.

Our controller, Figure 5a, uses this algorithm with two additions: offsetting and an iteration cap, now called Move Measure Offset Correct (MMOC). The controller stops if the error is within the given position and orientation tolerances, or if the iteration cap is reached. If required to meet tolerances, the iteration cap can be disabled. Once stopped, the Software Defined Triggering (SDT) is ran to capture data. The controller can fail if the UR10's collaborative safety system is triggered, if CD anticipates a move will cause a collision, or if the software crashes. Restarting allows for the PLGRM system to recover from any fault without losing progress.

Offsetting is indicated in Figure 5a. The previous point's corrections are accumulated and used to offset the next point. The assumption being made is that neighboring points will have similar corrections, possibly due to modeling errors. The benefit of offsetting is seen in 5b where the dominant number of corrections, four for MMC, goes to zero with offsetting. This saved a significant amount of time, reducing the time spent per point, including SDT, to a maximum of one second.

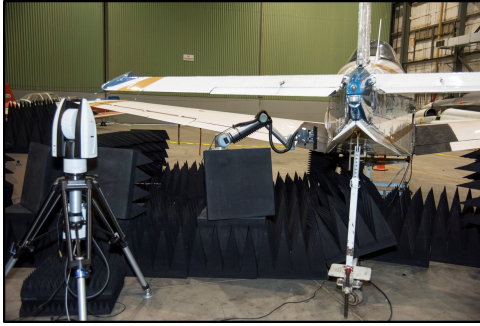


(a)

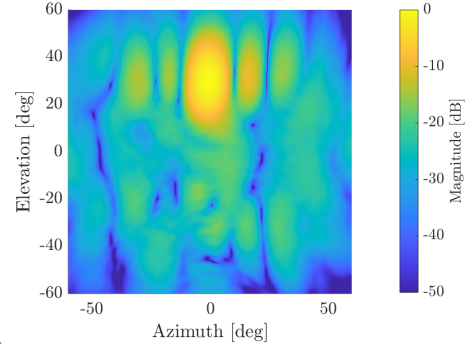


(b)

Fig. 6: Far-field configuration. Two robot positions were used, one with the LIFTKIT lowered to get most points, and one raised to capture the main beam. Both required moving the robot back to be on a 1.7 meter radius arc. Results in 6b for five phased array states were captured simultaneously using SDT to reprogram the array at each point.



(a)



(b)

Fig. 7: Planar near-field configuration. The robot was positioned closer to the aircraft and the LIFTKIT lowered for a 0.5824 meter by 0.4667 meter rectangular scan with 57x46x2 (5244) points and a 3λ AUT offset at 14.25 GHz. Figure 7b is the far-field antenna pattern from the transformed near-field data.

There are three sources of error to consider in the controller. The first is modeling error, the uncertainty of the parameters used in IK calculations. This can almost be eliminated by calibrating the robot [8]. The second is external disturbances that cause robot movement errors and they cannot be eliminated. Finally, the published laser tracker measurement accuracy, a maximum of $\pm(15\mu\text{m} + 6\mu\text{m}/\text{m})$ for position, and the orientation is typically within ± 0.01 degrees [12].

Controller performance was analyzed for a 5244 point near-field scan, Figure 5. The 200 micron position tolerance was chosen by the $\lambda/100$ metric for planar near-field scanning at 14.25 GHz [9]. The iteration cap was set at five to balance accuracy and time. Most points met the tolerance, as indicated in 5c, where about four percent of points were iteration capped.

The orientation error, Figure 5d, is the rotation required to get the probe antenna to the desired orientation. We can interpret it in maximum mechanical cross-polarization error (MMCPE).

Assuming that disturbances effect both orthogonal polarizations independently, the maximum error occurs when the disturbances oppose each other. For our mean value of 19.01 millidegrees, and with the typical orientation measurement accuracy of 10 millidegrees, the MMCPE is then $10 \log_{10}[\text{tand}[2(19.01\text{e}-3 + 10\text{e}-3)]] \approx -29.95$ dB. This was determined to be sufficiently small for our application.

The position and orientation errors are known to the limit of laser tracker accuracy, and can be corrected using algorithms such as the fast irregular antenna field transformation algorithm (FIAFTA) [17]. Advanced controllers and algorithms will be explored to properly account for these errors and enable faster, higher accuracy measurements.

F. Software Defined Triggering

SDT is the idea that data acquisition should be accomplished using software written in high level programming languages. At each point, a set of user provided software is called in the order given. This makes the PLGRM system easily adapted to new types of measurements.

SDT allows for the VNA to be substituted based on availability and the desired weight. This is accomplished through a generic SCPI driver for control of the two VNA models. Figure 6b demonstrates an example where five phased array states are measured simultaneously. Software was written to cycle through the five states and capture a VNA measurement at each. Removing the repeated robot movements significantly reduced the total measurement time compared to five separate FF measurements. It also benefited comparison between states, as they had the same probe antenna position and orientation. Future work will explore how SDT can be applied to continuous scanning while maintaining accurate position, orientation, and timing.

IV. RESULTS

The PLGRM system was deployed at NASA's Armstrong Flight Research Center for a week. It took a day to mount the AUT on the aircraft and setup the PLGRM system. Three near-field scans at 90 minutes each and various far-field cuts, taking a few minutes each, were collected over three days. On the final day, the PLGRM system was repacked for shipping back to Glenn Research Center. More details on the AUT and measurements are provided in another paper [18].

Here, example results for both a far-field (Figure 6) and a near-field (Figure 7) measurement are provided. The first measurements were FF cuts along a 1.7 meter arc and had to be captured in two robot positions, Figure 6b. Only the LIFTKIT was used to alternate between them so each measurement was quick. Once it was verified that the AUT was functioning, NF scans were performed to collect more complete data, Figure 7b. The NF scans occurred lower and closer to the aircraft, as seen by the different robot positions in Figures 6a and 7a. The measurements validated the AUT functionality prior to flight testing.

V. CONCLUSION

The design of the PLGRM system has been presented and discussed. Initial results demonstrate the viability of the PLGRM system for antenna measurements at Ku-band. The next steps are to reduce measurement time and increase accuracy as mentioned in each section. Additionally, RF absorber placement and cable management will be studied to better understand how they are affected by robotic antenna measurements. Finally, possible uses of the PLGRM system outside of antenna measurements will be explored, such as for robotic CNC machining [19].

ACKNOWLEDGMENT

The team would like to acknowledge the support of the Convergent Aeronautics Solutions project under Aeronautics Research Mission Directorate. The author, Peter Slater, would like to thank his mentors: James Downey, Marie Piasecki, and Bryan Schoenholz for their guidance during this project.

REFERENCES

- [1] A. Geise, O. Neitz, J. Migl, H. Steiner, T. Fritzel, C. Hunscher, and T. F. Eibert, "A crane-based portable antenna measurement system—system description and validation," *IEEE Transactions on Antennas and Propagation*, vol. 67, no. 5, pp. 3346–3357, May 2019.
- [2] D. R. Novotny, J. A. Gordon, M. S. Allman, J. R. Guerrieri, and A. E. Curtin, "Three antenna ranges based on articulated robotic arms at the national institute of standards and technology: Usability for over-the-air and standard near-field measurements," in *2017 IEEE Conference on Antenna Measurements Applications (CAMA)*, Dec 2017, pp. 1–4.
- [3] J. Hatzis, P. Pelland, and G. Hindman, "Implementation of a combination planar and spherical near-field antenna measurement system using an industrial 6-axis robot," in *AMTA 2016 Proceedings*, Oct 2016, pp. 1–6.
- [4] R. M. Lebrón, J. L. Salazar, C. Fulton, S. Duthoit, D. Schmidt, and R. Palmer, "A novel near-field robotic scanner for surface, rf and thermal characterization of millimeter-wave active phased array antenna," in *2016 IEEE International Symposium on Phased Array Systems and Technology (PAST)*, Oct 2016, pp. 1–6.
- [5] L. Boehm, S. Pleidl, F. Boegelsack, M. Hitzler, and C. Waldschmidt, "Robotically controlled directivity and gain measurements of integrated antennas at 280 ghz," in *2015 European Microwave Conference (EuMC)*, Sep. 2015, pp. 315–318.
- [6] N. Petrovic, T. Gunnarsson, N. Joachimowicz, and M. Otterskog, "Robot controlled data acquisition system for microwave imaging," in *2009 3rd European Conference on Antennas and Propagation*, March 2009, pp. 3356–3360.
- [7] D. R. Novotny and J. A. Gordon, "Practical considerations when using commercial robotic arms for antenna metrology," in *2018 International Symposium on Antennas and Propagation (ISAP)*, Oct 2018, pp. 1–2.
- [8] S. Droll, "Real time path correction of industrial robots with direct end-effector feedback from a laser tracker," *SAE International Journal of Aerospace*, vol. 7, no. 2, pp. 222–228, Sep. 2014. [Online]. Available: <https://doi.org/10.4271/2014-01-2248>
- [9] D. R. Novotny, J. R. Guerrieri, and J. A. Gordon, "Antenna alignment and positional validation of a mmwave antenna system using 6d coordinate metrology," *2014 Proceedings of the Antenna Measurement Techniques Association*, Oct 2014.
- [10] "Universal robot ur10." [Online]. Available: <https://www.universal-robots.com/products/ur10-robot/>
- [11] A. Yaghjian, "An overview of near-field antenna measurements," *IEEE Transactions on Antennas and Propagation*, vol. 34, no. 1, pp. 30–45, January 1986.
- [12] "Leica absolute tracker at960." [Online]. Available: <https://www.hexagonmi.com/products/laser-tracker-systems/leica-absolute-tracker-at960>
- [13] "Geodetic systems inc. v-stars n." [Online]. Available: <https://www.geodetic.com/products/systems/v-stars-n/>
- [14] S. Gottschalk, M. C. Lin, and D. Manocha, "OBTree," in *Proceedings of the 23rd annual conference on Computer graphics and interactive techniques - SIGGRAPH96*. ACM Press, 1996. [Online]. Available: <https://doi.org/10.1145/237170.237244>
- [15] K. P. Hawkins, "Analytic inverse kinematics for the universal robots ur-5/ur-10 arms," Dec 2013. [Online]. Available: <https://smartech.gatech.edu/handle/1853/50782>
- [16] M. S. Allman, D. R. Novotny, J. A. Gordon, A. Curtin, and S. Sandwith, "Serial robotic arm joint characterization measurements for antenna metrology," *2017 Proceedings of the Antenna Measurement Techniques Association*, Oct 2017.
- [17] C. H. Schmidt, M. M. Leibfritz, and T. F. Eibert, "Fully probe-corrected near-field far-field transformation employing plane wave expansion and diagonal translation operators," *IEEE Transactions on Antennas and Propagation*, vol. 56, no. 3, pp. 737–746, March 2008.
- [18] M. T. Piasecki, P. A. Slater, J. M. Downey, B. L. Schoenholz, and K. M. Lambert, "Active array measurements using the portable laser guided robotic metrology system," *2019 Proceedings of the Antenna Measurement Techniques Association*, Oct 2019.
- [19] C. Brillinger, H. Susemihl, F. Ehmke, T. Staude, K. Deutmarg, M. Klemstein, C. Boehlmann, W. Hintze, and J. Wollnack, "Mobile laser trackers for aircraft manufacturing: Increasing accuracy and productivity of robotic applications for large parts," in *SAE Technical Paper*. SAE International, 03 2019. [Online]. Available: <https://doi.org/10.4271/2019-01-1368>